Catalysis Communications 23 (2012) 62–66

Contents lists available at SciVerse ScienceDirect

Catalysis Communications

journal homepage: www.elsevier.com/locate/catcom

Short Communication

Inverse rod-like CeO_2 supported on CuO prepared by hydrothermal method for preferential oxidation of carbon monoxide

Shanghong Zeng, Wenli Zhang, Suilin Guo, Haiquan Su *

Inner Mongolia Key Laboratory of Chemistry and Physics of Rare Earth Materials, School of Chemistry and Chemical Engineering, Inner Mongolia University, Hohhot 010021, PR China

ARTICLE INFO

Article history:
Received 23 December 2011
Received in revised form 26 February 2012
Accepted 29 February 2012
Available online 6 March 2012

Keywords:
CeO_2/CuO
Rod
Particle
Hydrogen
CO-PROX

ABSTRACT

The CeO_2/CuO catalysts were synthesized by the hydrothermal method and characterized via XRD, BET, SEM, H_2-TPR, XPS and HRTEM techniques. The results showed that CeO_2 with two kinds of morphologies (particle and rod-like CeO_2) was highly dispersed on the surface of the catalysts when Ce/Cu molar ratio exceeded 0.25. The rod-like CeO_2 exposed more (1 1 1) planes, and this was helpful for oxygen storage and transportation. Moreover, the contact interface between highly dispersed CuO and bulk ceria supplied the active sites not only for CO oxidation but also for H_2 oxidation, but the contact interface of highly dispersed ceria and bulk CuO was more favorable for CO oxidation than H_2 oxidation.

1. Introduction

The preferential CO oxidation (CO-PROX) has recently attracted more interest as a final purification step of hydrogen feed gas due to the intense development of the proton-exchange membrane fuel cell (PEMFC) technology. The presence of 1 vol.% CO in the hydrogen stream will poison Pt anode of fuel cell, thus it is very essential to remove CO to a trace-level from the reformate stream. Among the current available methods, CO-PROX is the simplest and efficient approach for purifying hydrogen [1–6].

To date, catalysts used for CO-PROX mainly include platinum group metals (Pt, Pd, Ru, and Rh) catalysts, gold-based catalysts and transition metal-based catalysts (Co, Cu, and Mn) [7–9]. Among the catalysts, CuO/CeO_2 catalyst has been considered as a promising catalyst due to its low cost and high catalytic performance comparable to gold or platinum catalysts. It is generally accepted that the optimum catalytic performance over CuO/CeO_2 catalyst can be achieved under the condition of highly dispersed copper oxide patches over ceria nanoparticles [10–14]. In 2010 Martinez-Arias et al. [15,16], reported that the inverse CeO_2/CuO catalyst synthesized by the microemulsion method obtained wider CO conversion window and higher CO_2 selectivity than the traditional CuO/CeO_2 catalyst, indicating that it was the lower activity for H_2 oxidation reaction [17–22].

In this work, we reported the CeO_2/CuO catalysts prepared by hydrothermal method in order to study the mechanism of CO and H_2 oxidation over the CeO_2/CuO catalysts.

2. Experimental

2.1. Catalyst preparation

The CeO_2/CuO catalysts of different ratios (Ce/Cu molar ratio = 1:2, 1:4 and 1:10, respectively named as A, B and C) were prepared by the hydrothermal method. CTAB was dissolved in the deionized water, and 1.00 M $Cu(NO_3)_2 \cdot 3H_2O$ as well as 1.00 M $Ce(NO_3)_3 \cdot 6H_2O$ was added into the CTAB (Hexadecyl trimethyl ammonium Bromide) solution under vigorously stirring. Then $NH_3 \cdot H_2O$ was added dropwise to the above solution until the pH value of the mixture was adjusted to approximate 8.0. The solution became a gel and changed its color from colorless to dark blue. The obtained solution was transferred into a stainless steel autoclave with 120 ml-capacity teflon liner and heated for 24 h at 388 K. Finally, the catalysts after centrifuging, washing and drying were calcined at 773 K for 3 h at atmospheric pressure.

The same method was used to prepare the CeO_2/CuO-D, and the difference was that the pH value of the mixture was adjusted to 10.0. The CuO/CeO_2 catalyst was selected from our previous research [23].

2.2. Catalyst characterization

The scanning electron microscopy images of the samples were taken on a Hitachi S-3400N scanning electron microscope and the samples were coated with a thin layer of gold before scanning. X-ray diffraction patterns of the samples were carried on a MAC Science diffractometer equipped with a Cu Kα source and a power setting of 40 kV and 100 mA. TPR was performed in the 5% H_2/N_2 gas mixture on a TP-5080 instrument. The flow rate of the gas was 40 ml/min and the heating rate was 10 °C/min. The BET surface area and pore structure

---

* Corresponding author. Tel.: +86 471 4995006; fax: +86 471 4992981.
E-mail address: haiquansu@yahoo.com (H. Su).

1566-7367/$ – see front matter © 2012 Elsevier B.V. All rights reserved.
doi:10.1016/j.catcom.2012.02.028

of the catalysts were determined by nitrogen physisorption at liquid nitrogen temperature using a Micromeritics ASAP2020 Apparatus. High-resolution transmission electron microscopy (HRTEM) images of the catalysts were obtained on a JEOL 2010 transmission electron microscope. The X-ray photoelectron spectra of the samples were collected using a Physical Electronics Kratos Amicus spectrometer that were carried out under the requirement of UHV conditions with tapered anode Mg Kα radiation. The content of Ce and Cu was measured on an ICP-AES Spectrometer from American Varian Corporation.

2.3. Catalytic performance test

The catalytic oxidation of CO in hydrogen-rich gasses was carried in the quartz reactor. The reaction was operated between 35 °C and 215 °C at atmospheric pressure. The reaction mixture consisted of 1%CO, 1%O_2 and 50%H_2 (volume fraction) with N_2 as balance gas. The space velocity was 40,000 ml g_{cat}^{-1} h^{-1}. The inlet and outlet streams were measured using an on-line gas chromatograph (Shimadzu GC-8A) equipped with a thermal conductivity detector (TCD). The 5 A molecular sieve column was used to separate CO, O_2 and N_2. CO and CO_2 were determined by the TDX-01 column. The conversion of CO (C_{CO}) and the selectivity for CO oxidation (S_{CO}) were calculated according to Eqs. (1) and (2) [23]:

$$C_{CO} = ([CO]_{in} - [CO]_{out}) / [CO]_{in} \times 100\% \quad (1)$$

$$S_{CO} = 0.5([CO]_{in} - [CO]_{out}) / ([O_2]_{in} - [O_2]_{out}) \times 100\% \quad (2)$$

3. Results and discussion

3.1. Scanning electron microscopy

Fig. 1 showed the SEM micrographs of the CeO_2/CuO catalysts. It was obvious that CeO_2 had two kinds of morphologies in the images of CeO_2/CuO-A, CeO_2/CuO-B and CeO_2/CuO-D, including particle and rod-like CeO_2. The CeO_2 rods were 0.2–0.4 μm in lateral size and 0.5–1.5 μm in longitudinal direction, and the average diameter and length are 0.3 and 1.0 μm, respectively. But for CeO_2/CuO-C, only particle-like CeO_2 could be seen in Fig. 1C. It showed that the particle-like CeO_2 could self-assemble into the rod-like CeO_2 when the Ce/Cu molar ratio was ≥0.25. It was reported that the morphology-dependent phenomenon was closely related to the nature of the exposed crystal planes [24]. The rod-like CeO_2 nanostructures preferentially exposed the (1 1 0) and (1 0 0) planes, however, the CeO_2 nanoparticles mainly exposed the stable (1 1 1) plane on the surface.

3.2. X-ray powder diffraction

Fig. 2 showed XRD patterns of the inverse CeO_2/CuO catalysts. It could be seen that CuO existed in monoclinic phase and CeO_2 was cubic fluorite structure. For each CeO_2/CuO, only the weak diffraction peaks of (1 1 1), (2 0 0), (2 2 0) and (3 1 1) planes of CeO_2 could be seen at 28.69°, 32.48°, 47.48° and 56.54°, suggesting that CeO_2 was highly dispersed on the CuO supports. The CeO_2/CuO-C which was composed of the particle-like CeO_2 had highest CuO crystallinity because of low Ce/Cu molar ratio comparable to the other catalysts. From Table 1, the interplanar crystal spacing of CeO_2 over the CeO_2/CuO catalysts hadn't greatly changed comparable to CeO_2, indicating that Cu^{2+} didn't enter into the crystal lattice of CeO_2 although the radius of Cu^{2+} (72 pm) was smaller than that of Ce^{4+} (92 pm). But for CeO_2/CuO-D, the interplanar crystal spacing of CuO obviously became bigger comparable to single CuO, suggesting that Ce^{4+} entered into the crystal lattice of CuO, which could improve the interaction between CeO_2 and CuO and catalytic activity. The crystallite size was estimated by applying the Scherrer equation to the CeO_2 and CuO peaks in the XRD spectra of the catalysts. As shown in Table 1, the average particle size of CeO_2 increased with the decrease of Ce/Cu molar ratio when the pH value of solution was equal to 8. The average par-

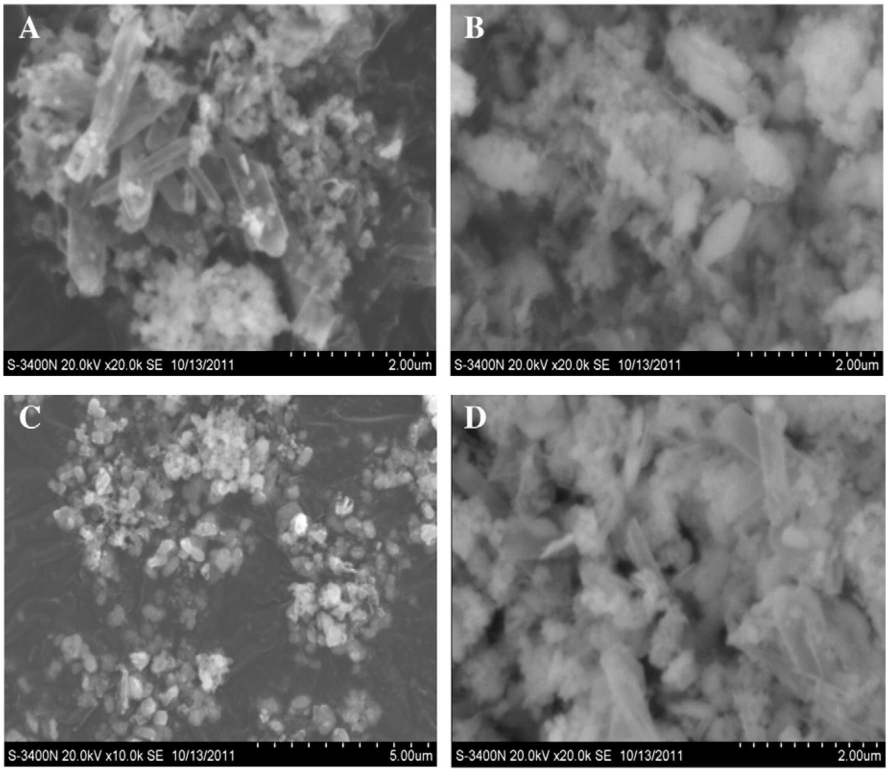

Fig. 1. SEM images of the catalysts: (A) CeO_2/CuO-A; (B) CeO_2/CuO-B; (C) CeO_2/CuO-C; (D) CeO_2/CuO-D.